Speckle removal in SAR data by wavelets

M. P. Sassano[1]

A.N. Proto[1,2*]

[1] *Laboratorio de Sistemas Complejos, Facultad de Ingenieria, Universidad de Buenos Aires*

[2] *Comision de Investigaciones Cientificas*
E-mail: aproto@fi.uba.ar

Abstract

A method for specckle removal in Synthetic Aperture Radar (SAR) images based on wavelets filters is presented. Our method is applied to SAR signals prevously to proceed to the imaging of the data. The spatial resolution and image details are strongly enhanced, without 'blurring' effects.

Key words: Synthetic Aperture Radar; Speckle removal; Data processing

Introduction

Synthetic Aperture Radar (SAR), is a remarkable device very useful for earth's observation [2–4]. It is a microwave remote sensing technique whose principal advantage comes from allowing high resolution measurements of the Earth surface in all weather conditions. The radar system send to Earth coherent frequency modulated, high energy pulses, called chirps, with a given pulse repetition frequency (PRF). The energy of the pulse propagates in the range direction, and the flight direction is defined as azimuth. The backscattered echoes are registered by the same emission-transmission antenna. Echoes, after analog/digital-conversions and compression are downloaded to another antenna at the ground segment, together with parameters referred to the acquisition mode and orbit definition. .The key point in SAR is to use a small antenna (10-12 M. in azimuth) to cover 70-100 Km on Earth surface. So, every point on the ground should be illuminated by thousands of pulses, in order to obtain the adequate response intensity. At the ground segment chirp echoes are decompressed and separated from parameters and then converted to raw data. These raw data are then used to produce a SAR image. There exist several

different algorithms for dealing with the SAR raw data to transform them into a SAR image [2–4]. all of them are based on the fact that the SAR system preserves the phase information and all received echoes in azimuth can be coherently combined after a proper phase correction.

Due to this particular measurement process involving many in flight chirps pulses [2–4], SAR images present a non desirable effect which is called speckle [5]. This effect is the consequence of the multiple interference patterns coming from of the chirp pulse illumination impinging on the different scatterers of a broad scene. There many different methods to remove speckle form SAR images, based on different procedures [5], and in last years, wavelet filtering procedures have been broadly used [6,7], and references therein. As we have explained before, SAR images are obtained from the SAR signals (raw data) after some procedure able to compensate the varying distance from the sensor to a point scatterer [2–4], the range cell migration correction, (RCMC).

The complete removal of speckle noise without losing relevant information in a SAR image is still an open problem. In general, filtering techniques usually remove also useful information meantime some residual speckle noise still remain. One of the most common problems appearing in even in the modern adaptive filters, like wavelets techniques applied on the SAR image, lead to a 'blurring 'effect. This problem is basically due to using local statistical information taken from the neighborhood of the pixel in analysis. besides, if edges are present the filtering process may lead to incorrect results. . Notice that at the present all the proposed techniques for speckle removal are applied on the SAR image.

In this paper, we propose a new concept to remove speckle, following a complete different route. We here deal with the raw data a step before the image, which is obtained from these data using an imaging procedure. The present approach improves speckle reduction, image quality, and edge sharpening in the subsequent SAR image.

Our main goal was to deal with the speckle contributions at *SAR raw data level,* Fig.2, where these contributions can be treated like 'noise', as raw data are a matrix composed by temporal signals. After removing this peculiar 'noise' from the SAR signal, we apply the phase correction,[8] improving the quality of the SAR image as we shall demonstrated below. *The procedure we are here presenting, demands a careful information processing of the raw data, in order to keep the original phase preserving ability of SAR systems.* Otherwise it would be impossible to get the corresponding SAR image.

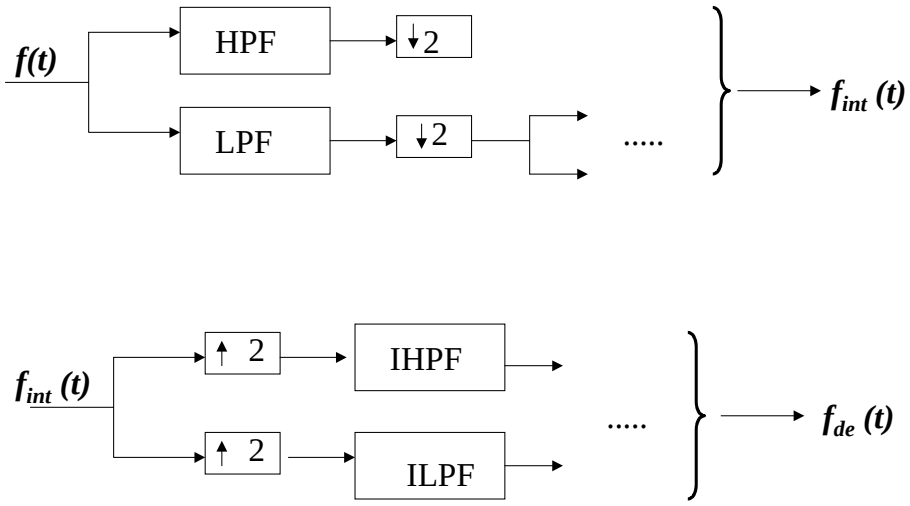

Fig. 1. The WDT filter bank

1 Brief review about wavelets de-noising technique (WDT)

A low pass filter greatly reduces the high frequency components, which often represent noise in the signal, being this is the guiding idea in many problems of signal analysis and synthesis. The main problem is to reconstruct the signal, removing noise, but not the relevant information. In general, the problem is solved using two filters, a high pass (HPF) as well as low pass filter (LPF). This process generates a "filter bank", which sends the signal trough two or more filters, normally structured in tree. Through the Discrete Wavelet Transform (DWT) and the Inverse Discrete Wavelet Transform (IDWT) it is possible to decompose and reconstruct the signal. In fact, the word "wavelet " is properly associated with a "multiresolution into different scales". The simplest change of scale comes from down sampling a signal keeping only its even –numbered components. This sampling operation is denoted by the symbol $(\downarrow 2)$, and it is possible to use different scales (fine, medium, and coarse). The overall filter bank Fig.1 is the successive application of the $(\downarrow 2)$operation, L times. In theory, L can be even infinite, but as in reality signals have finite length, necessarily the process can done up to the number of samples. So, the basic wavelet idea is to repeat the filter bank: the low pass output becomes the input to the second filter bank.

After the complete down-up filtering the f_{de} signal is obtained. The computation is cut in half because the input is decomposed by the HPF and the LPF. Typical applications of the wavelet transform go to four or five decomposition levels. This completes the iteration of the analysis bank in down sampling. The filtering followed by down sampling is inverted by up sampling $(\uparrow 2)$, followed by filtering. So, the process of filtering followed by down sampling is inverted by up sampling followed by filtering. The iteration process can be done due to the wavelets theory and filter banks connection developed in the 80' by Ingrid Daubechies [10]. In order of giving a brief idea of the method we are here using, we begin with the fundamental dilation equation or relation between scales also called refinement equation:

$$\Phi(t) = 2\sum_{k=0}^{N} h(k).\Phi(2t - k) \tag{1}$$

Eq.(1) is linear, and $\Phi(t)$ is called the scale function. If $\Phi(t)$ is a solution, so is any multiple of $\Phi(t)$ is a solution too. As usual the normalization condition is $\int \Phi(t)\,dt = 1$. The integral extends over all time, but it is possible to show that the solution $\Phi(t)$ is zero outside the interval $0 \leq t \leq N$ [10]. The scaling function has compact support, and the localization of the function is one of its most useful properties. The two key operations of classical wavelet theory are: Dilation of the time scale by 2 or 2^j, which means that the graph of $\Phi(t)$ is compressed by 2, and translation of the time scale by 1 or k, which means that the graph of $\Phi(t)$ is shifted by k. The combination of those operations, from to $2^j t$ to $2^j t - k$, will later produce a family of wavelets $\omega(2^j t - k)$ from a single wavelet . The scaling function is smoother and live in $\mathbb{L}^2(R)$. If the original input is a box function, we get $\Phi^{i+1}(t)$ from $\Phi^i(t)$, and the filter re-scale results:

$$\Phi^{i+1}(t) = 2\sum_{k=0}^{N} h(k).\Phi^i(2t - k) \tag{2}$$

where $h(k)$ are the decomposition coefficients. This operation is called the cascade algorithm, because the low pass filter is "cascaded" to different time scales. If this iteration converges, $\Phi^i(t)$ approaches to $\Phi(t)$ in the limit $t \longrightarrow \infty$ and then $\Phi(t)$ satisfies Eq.(1) or refinement equation.. Further improvement of the theory, can be obtained using Multiresolution Analysis (MRA).In this description, the refinement equation gives the limit of an infinite filter tree. MRA looks at different time scales, t and $2^j t$ for every t. This corresponds to octaves in the frequency domain. Multiresolution analysis works on two different and simultaneous scales: a time-scale, labeled by

j , and a position scale labeled by k. In order to give a brief description of the MRA, we need to introduce a succession of vectorial spaces where the $\Phi(t)$ scale functions belong to. We can construct an increasing sequence of spaces $V_0 \subset V_1 \subset ... \subset V_j \subset ..$The approximated space V_j contains all combinations of the shifted and compressed scaling function $\Phi(2^j t - k)$ $-\infty < k < \infty$. So, $V_0 \subset V_1$ and every $V_j \subset V_{j+1}$, as can be deduced directly looking at $\Phi(t) = 2\sum_{k=0}^{N} h(k).\Phi(2t - k)$. Let us now looking at the functions which are in V_1 but not in V_0. This will lead us to the "wavelet space W_0" composed as $V_1 = V_0 \oplus .W_0$ .As in general, $W_j \subset V_{j+1}$, $W_j \perp V_{j+1}$and $W_j \oplus V_{j+1}$,then, it results that $\mathbb{L}^2 = V_0 + W_0 + W_1 + ...$So, any finite-energy function $f(t)$ can be decomposed into the succession of V_j spaces in terms of the corresponding $\Phi^j(t)$. Suppose that the functions $\Phi(2^j t - k)$ are orthogonal. We will write:

$$f(t) = f_0(t) + [f_1(t) - f_0(t)] + [f_2(t) - f_1(t)] + ... \tag{3}$$

This is the sum of a lowest-level "coarse function" $f_0(t)$ and an infinite series of "fine details" $d_j = f_{j+1}(t) - f_j(t)$, where the $d_j \in W_j$. As $f_j(t)$ is the projection of $f(t)$ into V_j ,then $f(t) - f_j(t)$ is also orthogonal to V_j and analogously, $f(t) - f_{j+1}(t)$ is orthogonal to V_{j+1}, and therefore to V_j. Then $d_j = f_{j+1}(t) - f_j(t)$ is orthogonal to V_j. The central point of MRA is to make that the details d_j result to be a combination of compressed-translated $\omega(2^j t - k)$, which form the basis of W_j . The fundamental detail function $\omega(t)$ will be then a wavelet of the form:

$$\omega(t) = 2\sum_{k=0} h_1(k).\Phi(2t - k) \tag{4}$$

because $W_0 \subset V_1$,where the $h_1(k)$ are wavelets coefficients and $\omega(t)$ is the mother wavelet. The wavelet coefficients $h_1(k)$ produce a "scalogram" instead of a spectrogram. Further details of the method can be found in (Mallat, 1998). The relationship between the low pass and high pass filters are: $h_1(k) = (-1)^k h_0(N - k)$, and using this property of the coefficients, we can prove that $\omega(t)$ is orthogonal to $\Phi(t)$.according to this we can write:

$$f(t) = \sum_k c_{jk}\Phi_{jk} + \sum_k d_{jk}\omega_{jk} \tag{5}$$

where $c_{jk} =< f(t), \Phi_{jk} >$ and $d_{jk} =< f(t), \omega_{jk} >$,taken into account the orthogonality properties of the basis into the corresponding spaces. I

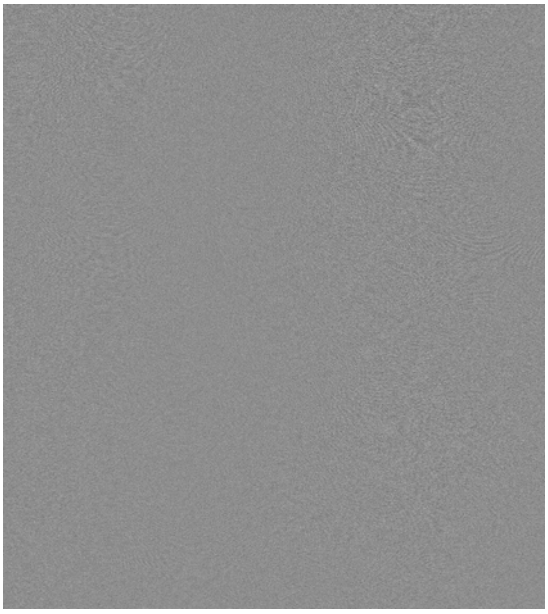

Fig. 2. Bidensional representation of SAR signals

2 SAR case

In this section we will show the results we have obtained for the SAR signals and how these results enhance the subsequent SAR image. The real signals and images shown in this work corresponds to an ERS-2 SAR acquisition data set corresponding to the Buenos Aires City area, taken at the CONAE Teofilo Tabanera Ground Station on August 5, 1997 (Full area quick look at www.conae.gov.ar ; Track/Frame: 11981/6489; Hour: 03:01:21.032; Localization: (1) Lat.: -34(S.) 15' 12" - Lon: -59(W.) 14' 03", (2) Lat.: -34(S.) 00' 45" - Lon: -58(W.) 10' 58", (3) Lat.: -35(S.) 08' 16" - Lon: -58(W.) 57' 20", (4) Lat.: -34(S.) 53' 40" - Lon: -57(W.) 53' 27"). The ERS-2 raw data is a matrix of 5616 complex samples and 27200 lines.

2.1 SAR signals

In order to show the nature of the SAR signals, in Fig.2 we show a bidimesional (matricial) representation of the raw data, where rows are SAR signals sampled in slant range, and columns are the different received echoes, which provide the sampling in azimuth direction. Each line of the matrix is in fact a temporal signal, sampled according to the sampling frequency, defined by the Ers-2 SAR apparatus measurement process (Fig.2). The raw data are, in fact, a collection of sampled signals ordered into a matrix, as result of the complex measurement method. For further details concerning SAR systems and its measurement process we refer the reader to [2–4,9].

In the present work, as we have said before, we take advantage of the special form of the SAR measurement process, to remove the speckle directly on the raw data (Fig.2) instead of doing it from the SAR image, using WDT directly onto temporal signal. In order to do so, we implemented a dyadic filter tree, as it can be seen in i.e. [11]. The input (initialization, [11]) to the filter bank, $f(t)$, is the subsequent 27200 files of the original SAR signals, and the signals are passed through a series of low-pass filters (LPF) and high-pass filters (HPF) as we have indicated in the preceding section. In order to make the calculations the filters are represented through two Toeplitz matrices, H (HPF) and G (LPF). After each filter, the signal is down sampled by $(\downarrow 2)$. The result of the filter bank, Eq.(5) is a set of scaled $c_{jk} = [H * c_{j+1}] \downarrow 2$ and wavelet $d_{jk} = [G * d_{j+1}] \downarrow 2$ coefficients . In (Fig.3) the complete procedure is shown.

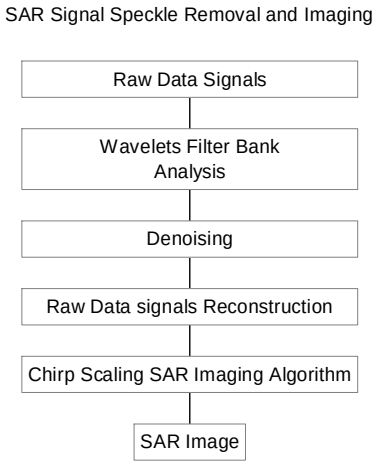

Fig. 3. Flow chart of the speckle removal in SAR images procedure

As it is well-known, filters are dependent on the selection of the $\omega(t)$ wavelet function, used in the transform. Then, the wavelet coefficients vary according to the selection of the mother wavelet $\omega(t)$. We have investigated a variety of mother wavelets in order to obtain the more efficient and adequate 'noise' (speckle) removal. As we have said above to be used in a filter bank, a mother wavelet function must satisfy the mutiresolution analysis (MRA). In our work we have used Daubechies-n wavelet, with $n = 4, 12$,and 20. The Daubechies wavelet has compact support, and the support length is $2n + 1$. Also the cubic Spline wavelet was used. After obtaining the down sampled intermediate signal $f_{int}(t)$ it is necessary to reconstruct the SAR signal data to proceed to obtain the SAR image. So, $f_{int}(t)$ is up sampled and filtered disregarding the lowest d_{jk} values by hard thresholding [11]. Then we applied an up sampling filter where $f_{int}(t)$ is the input. The output is the de-noised (de-speckled) raw

signal $f_{de}(t)$. The IHPF and the ILPF filters are represented by the Toeplitz matrices, $H_1$and G_1,and the coefficients for the reconstruction of the signal are: $c_{j+1} = ([c_j] \uparrow 2) * H_1 + ([d_j] \uparrow 2) * G_1$ .One of the most conflictive points in speckle removal is how many real information is also removed by the applied procedure. In order to measure the quality of our method, the degree of information removal is evaluated through the Shannon and the wavelet entropy., given by:

$$S = -\sum_{I=1}^{N} P(I) \ \ln \ (P(I)) \tag{6}$$

where $P(I)$ is the probability evaluated over the normalized signal as the value at each point divided by the summa of all points, and the Wavelet entropy [12] , S_{wt} given by:

$$S_{WT} = -\sum_{j<0} P_j \ \ln \ (P_j) \tag{7}$$

where $p_j = \frac{E_j}{E_{tot}}$ and

$$E_j = \sum_k \mid c_j(k) \mid^2 \wedge E_{tot} = \sum_{j<0} E_j \tag{8}$$

In order to clearly show our procedure, let us first applied the WDT to a simple ideal SAR chirp where an additional 30% of uniformly distributed random noise is added (see Fig.4). The de-noising is made using Daubechies-4 wavelets, and removing for the reconstruction the fourth level, which means we are doing a hard threshold de-noising. In Fig.4 we show: a) the noisy original chirp, b) the reconstructed denoised chirp. In Table I, the results for the chirp case, are given. IC means ideal chirp, and R means reconstruction.

As it can be seen, the Shannon entropy, S, tells us that we removed around a 1% of information, and S_{wt}, means that we keep after the reconstruction, around 72% of the original information, when comparison between column 2 and 4 is done. So, the amount of information removed by WDT is 2% less than the noise we have introduced into the signal (30%).

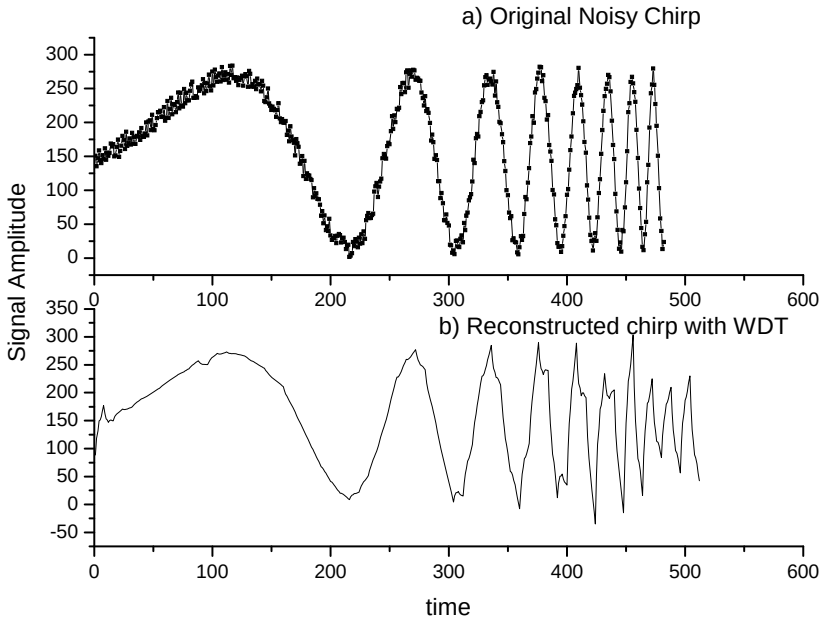

Fig. 4. Simulated FM chirps, as used in SAR technique, with 30% uniformly distributed random noise.

TABLE I	I C without noise	I C 30% noise	Perfect R	Denoised R
S	6.0123601	6.05999	6.05999	6.11681
S_{Wt}	0.766380	0.846791	0.84671	0.637014

Same information evaluation process was done for measured ERS-2 SAR signal (see details about the acquisition above) shown in Fig.5 which is a row of Fig.2. Fig.6 shows only a small portion of the original, $f(t)$, and the WDT denoised-reconstructed signals, $f_{de}(t)$,in order that details can be seen.

In Table II we give the information amount of an original ERS-2 SAR signal (one row of (Fig.2), the perfect reconstructed and the WDT signal information . In the WDT case S. indicates that we have removed 1% of information, and S_{wt}, the information removal with the same procedure as we done in the previous case is around 20%.

TABLE I I	Original SAR signal	Perfect R	Denoised R
S	8.5555413	8.55554	8.56579
S_{Wt}	1.20474	1.20474	0.963279

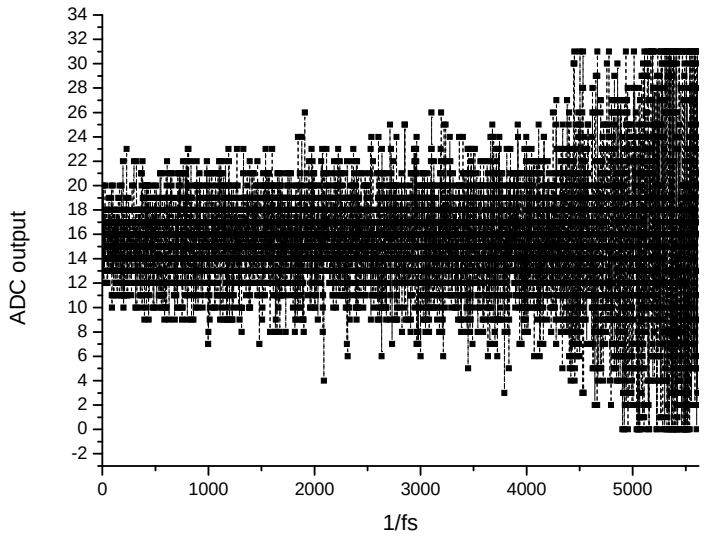

Fig. 5. One file of the raw data matrix (ADC output in 32 bits). Saturated data from corresponds to the town area, and the others to the River Plate zone.

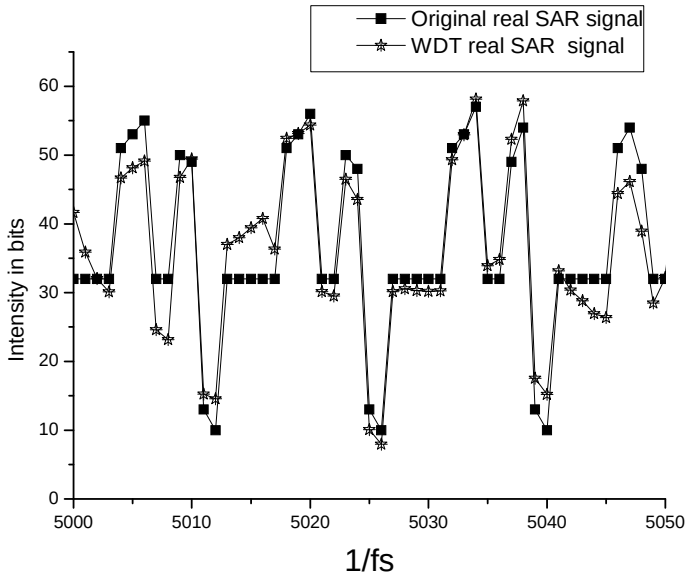

Fig. 6. Few points (50) of a ERS-2 SAR signal (5616). Squares points belong to the original SAR signal, and stars points belong to the reconstructed WDT SAR signal.

By comparison with the case of the simulated chirp, we can infer that for the SAR signal case, we are removing a 20% of the original signal. However, the final conclusion about the WDT for speckle removal in SAR images will be given after the imaging procedure. The mayor problem at the imaging step is to deal with a large amount of datacondering that each signal is wavelet

decomposed, de-noised and reconstructed. In the next Section we will present our results.

2.2 SAR images

After de-noising the SAR signal raw data, and recompose it using the procedure described in the previous Sections, we proceed to 'focalized' the signal. using the chirp scaling algorithm as derived in [8].

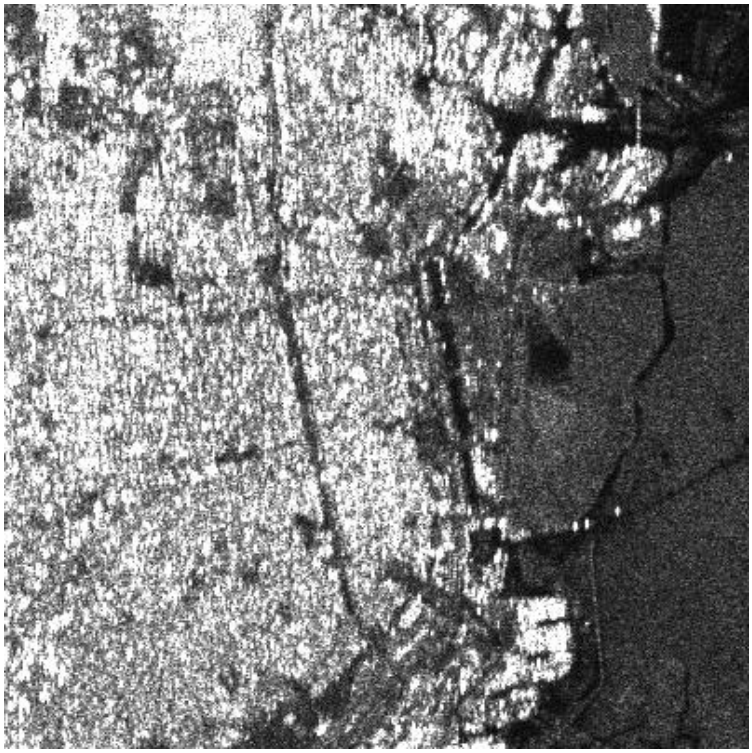

Fig. 7. Downtown area of the Buenos Aires City, obtained from Fig.2 , after applying the chirp scaling imaging procedure, without WDT denoising on the raw data (Fig.2).

In Fig.7 we show a subset of the image obtained from the data shown in Fig.2, without applying WDT after applying the chirp scaling imaging procedure [8]. In Fig.7, the high reflectivity of the city reinforce the speckle effects. Below we will show the same area with WDT.

As it can be seen by inspection, the downtown area is more clearly seen, and details of the streets can be observed. The shown area corresponds to a portion (around 4.5×4.5 Km) of a 100 ×100 Km image. More impressive are Fig.9 and Fig.10, where a set of buildings in the Buenos Aires City suburban area can be observed without and with WDT procedure.

In Fig.11 and Fig.12 we show zoom of the previous images, where the differ-

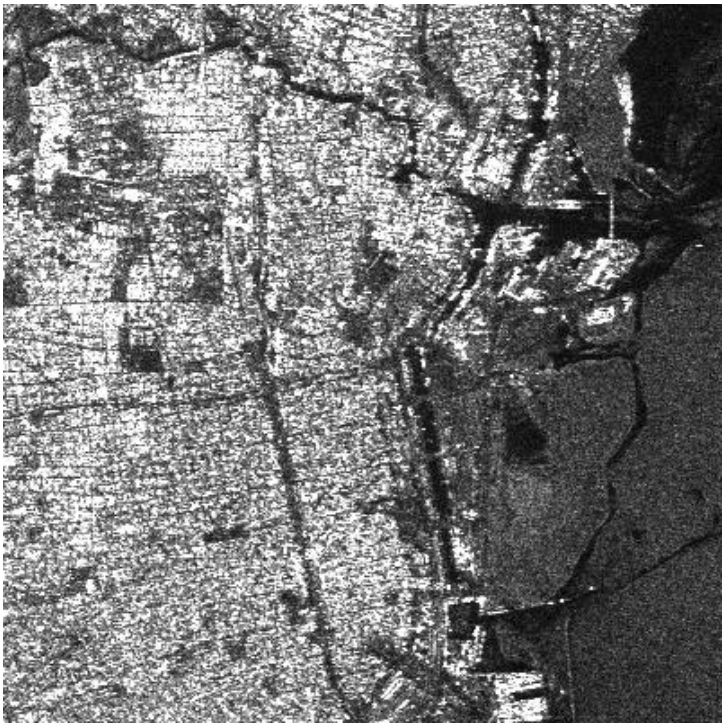

Fig. 8. Same portion as in Fig.7, where denoising on raw data was done before imaging procedure.

Fig. 9. Buenos Aires City suburban area, without WDT.

ences in the definition of the observed objects, in the present case, buildings, can be more clearly observed.

Fig. 10. Same area as in Fig.9 with WDT.

Fig. 11. An array of buildings from the Buenos Aires suburban area, without WDT

3 Conclusions

We present a method to remove speckle from SAR images, based on treating the speckle as noise. The information processing of the speckle was not doing at level image, but in a previous step, the SAR raw data. These data are an ordered succession of sampled signals which bidimensional representation can be seen in Fig. 2. At this level wavelet signal de-noising techniques can

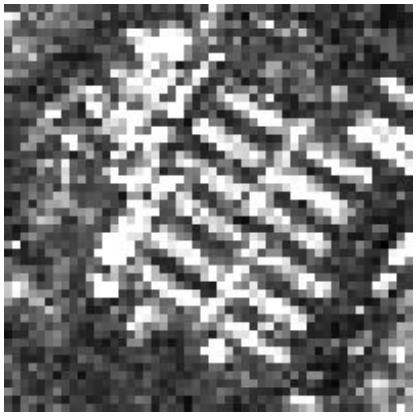

Fig. 12. The same area as in Fig.11, from the WDT treated SAR image.

be applied. The main goal of our method was to develop a data handling procedure able to remove the speckle keeping the phase preserving nature of SAR systems, which allows the image formation, as well as to give a measure of the information content of the denoised signals. Filters are represented by Toeplitz matrices, in the computational treatment. After the de-noising procedure, the phase correction is applied as was outlined before. The results shown in the figures speak by themselves and demonstrate the improvements we have obtained in the SAR image quality.

References

[1] Corresponding Author: LSC, FI-UBA, Av. Paseo Colon 850 4to Piso (1063) Buenos Aires Argentina

[2] Franceschetti, G. and Lanari, R. (1999) Synthetic Aperture Radar Processing, CRC Press LLC

[3] Curlander, J.C. and McDonough (1991) Synthetic Aperture Radar Systems and Signal processing. John Wiley and Sons, Inc.

[4] Carrara, W.G., Goodman, R.S. and Majewski, R.M., Spotlight Synthetic Aperture Radar, Signal processing and algorithms.Artech House,1995

[5] Oliver, C. and Quegan, S. (1998) Understanding Synthetic aperture Radar Images' Artech House Inc.

[6] Achim, A. Tsakalides, P. and Bezerianos, A. (2003) SAR Image Denoising via Bayesian Wavelet Shrinkage Based on Heavy-Tailed Modeling, IEEE Trans. on Geosci and Remote Sensing 41, 1773-1784.

[7] Sveinsson, J. R., and Benediktsson, J. A. (2003) Almost Translation InvariantWavelet Transformations for Speckle Reduction of SAR Images, IEEE Trans on Geosci. and Remote Sensing, 41, 2404-2408

[8] Raney, R.K., Runge, H. Bamler, R. Cumming, I.G., and Wong, F.H. (1994) IEEE Trans. on Geosci and Remote Sensing **32** 786-799

[9] Eldhuset,K., (1998) IEEE Trans. on Aerospace and Electronic Systems vol. 34 824-835

[10] Daubechies, I. (1992) Ten lectures on Wavelets' SIAM, Philadelphia, PA.

[11] Mallat, S. (1998) A wavelet Tour of Signal Processing', Academic Press Second Edition.

[12] Rosso, O., Blanco, S., Yordanova, J., Kolev, V., Figliola, A., Schurmann, M., Basar, E. (2001) Elsevier, Journal of Neuroscience Methods 105, 65-75.